

Compact InAlAs–InGaAs Metal–Semiconductor–Metal Photodetectors Integrated on Silicon-on-Insulator Waveguides

Joost Brouckaert, *Student Member, IEEE*, Gunther Roelkens, *Student Member, IEEE*,
Dries Van Thourhout, *Member, IEEE*, and Roel Baets, *Fellow, IEEE*

Abstract—We present measurement results of compact and efficient InAlAs–InGaAs metal–semiconductor–metal photodetectors integrated on silicon-on-insulator (SOI) waveguides. These thin-film devices are heterogeneously integrated on the SOI substrate by means of low-temperature die-to-wafer bonding using divinyl-disiloxane benzocyclobutene (DVS-BCB). The responsivity of a 30- μm -long detector is 1.0 A/W at a wavelength of 1550 nm and the dark current is 4.5 nA at a bias voltage of 5 V.

Index Terms—Heterogeneous integration, photodetector, photonic integrated circuit, silicon-on-insulator (SOI).

I. INTRODUCTION

SILICON photonics has gained a lot of popularity in recent years. This trend is fueled by several factors and research developments. The high refractive index contrast of the silicon-on-insulator (SOI) material system enables very compact and high density passive waveguide circuits. Moreover, these circuits can be fabricated using wafer scale complementary metal–oxide–semiconductor processing techniques resulting in low cost, high volume, and compact photonic integrated circuits [1].

For some optical functionalities, however, like amplification, generation, and detection of light at telecom wavelengths (1.3–1.55 μm), silicon is outperformed by III–V semiconductor materials: InGaAs, for example, has an unchallenged position in high speed, low dark current, and high sensitivity near-infrared photodetectors. These III–V materials can be heterogeneously integrated on an SOI wafer by means of a low-temperature die-to-wafer bonding process [2] and photodetectors, amplifiers, and laser diodes could be fabricated in the same processing steps, using wafer scale III–V technologies [3].

In this letter, we report a compact InAlAs–InGaAs metal–semiconductor–metal (MSM) photodetector coupled with an SOI waveguide. MSM detectors offer some advantages

Manuscript received April 26, 2007; revised June 20, 2007. This work was supported in part by the Institute for the Promotion of Innovation through Science and Technology (IWT Vlaanderen) under the SBO eSOC Project, by the IST Network of Excellence ePIXnet, and by the Interuniversity Attraction Poles (IAP)-Photon Network. The work of G. Roelkens was supported by the Fund for Scientific Research (FWO).

The authors are with the Department of Information Technology (INTEC), Ghent University-Interuniversity Microelectronics Center (IMEC), B-9000 Gent, Belgium (e-mail: joost.brouckaert@intec.ugent.be; gunther.roelkens@intec.ugent.be; dries.vanthourhout@intec.ugent.be; roel.baets@intec.ugent.be).

Digital Object Identifier 10.1109/LPT.2007.903767

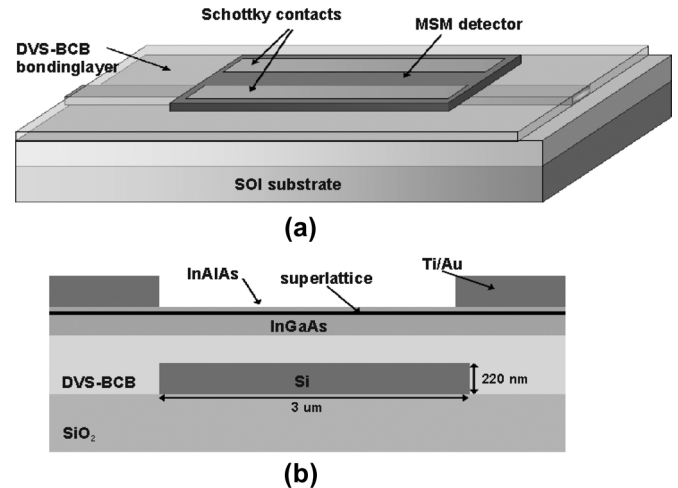


Fig. 1. (a) Three-dimensional and (b) cross-sectional schematic view of the waveguide integrated MSM detector.

as compared to pin detectors: the planar structure reduces the number of processing steps and their low capacitance per unit area makes them especially suitable for electronic circuits requiring a low input capacitance.

The heterogeneous integration of III–V on SOI starts with bonding unprocessed III–V dies (epitaxial layers down) onto a processed SOI waveguide wafer using low-temperature divinyl-disiloxane benzocyclobutene (DVS-BCB) bonding [2]. This is the only nonwafer scale process within the integration procedure, but as these dies are unprocessed, the alignment is not critical and a fast pick-and-place routine can be used. After bonding, the InP substrates are removed, obtaining defect-free epitaxial III–V films bonded onto a processed SOI substrate. Subsequently, the photodetectors are defined using wafer scale processes and lithographically aligned to the underlying SOI waveguides.

II. DESIGN AND FABRICATION

A. Device Structure and Design

The schematical view of the thin-film MSM detector is shown in Fig. 1. Detailed simulation results [4] and a preliminary measurement result [5] are discussed in other papers. In this letter, we discuss the fabrication and the performance of the component in more detail. The operation principle of the detector is based on directional coupling. By making use of a thin DVS-BCB bonding layer and by proper design to obtain

phase-matching between the optical mode in the SOI waveguide and the detector waveguide, optical coupling between both modes will occur. The SOI wafer consists of a 220-nm-thick Si layer on top of a 1- μm -thick SiO_2 buried oxide layer on a Si substrate. The SOI waveguide is etched through and is 3 μm wide. The detector layer structure consists of a 40-nm InAlAs Schottky barrier enhancement layer, 20-nm InAlAs–InGaAs digital graded superlattice layer to decrease carrier trapping by the bandgap discontinuity between $\text{In}_{0.52}\text{Al}_{0.48}\text{As}$ and $\text{In}_{0.53}\text{Ga}_{0.47}\text{As}$, and a 145-nm $\text{In}_{0.53}\text{Ga}_{0.47}\text{As}$ absorption layer. All layers are not intentionally doped and lattice-matched to the InP substrate. Two Schottky electrodes (Ti–Au, 20 nm/200 nm) are deposited on top, with a spacing equal to the SOI waveguide width, as can be seen in Fig. 1. Lateral confinement of light in the thin-film detector waveguide is obtained by the two coplanar Ti–Au Schottky contacts. The large imaginary parts of the refractive index of Ti (4.62) and Au (9.81) at a wavelength of 1.55 μm lowers the effective refractive index of these two vertical slices as compared with the central slice and this provides lateral confinement. As these two coplanar Schottky contacts are used to obtain lateral waveguide confinement, optical loss due to absorption in these contacts is limited and calculated to be less than 10% [4].

The advantage of this waveguide MSM geometry as compared to a normal incidence heterogeneously integrated pin photodetector design [6] is that it allows independent optimization of optical path length and carrier transit time. This transit time can be decreased by decreasing both SOI waveguide width and Schottky contact spacing. Using standard optical contact lithography, contact spacing of 1 μm is easily obtainable resulting in an estimated transit time limited bandwidth of 15–20 GHz as compared to literature examples [7]. A heterogeneously integrated edge-coupled pin photodetector [8] also allows efficient and high-speed operation but the need of an inverted SOI taper makes this device large as compared with the MSM detector reported in this letter.

B. Fabrication

The fabrication starts with the DVS-BCB die-to-wafer bonding. After cleaning, an unprocessed III–V die is bonded on top of the SOI waveguide substrate by means of DVS-BCB. The spacing between III–V and SOI is ~ 100 nm as can be seen in the cross section (Fig. 2). After bonding, the InP substrate is removed by grinding down to 60 μm and afterwards chemically etched using HCl until an InGaAs etch stop layer is reached. This etch stop layer on top of an InP sacrificial layer is removed by a selective wet etch using $\text{H}_2\text{SO}_4 : \text{H}_2\text{O}_2 : \text{H}_2\text{O}$ and finally, the InP sacrificial layer on top of the 40-nm InAlAs barrier enhancement layer is removed using 1 : 1 : 2 HCl : H_3PO_4 : CH_3COOH . The detector area is defined by etching down to the DVS-BCB bonding layer by means of nonselective wet etching using 1 : 1 : 20 $\text{H}_3\text{PO}_4 : \text{H}_2\text{O}_2 : \text{H}_2\text{O}$. In a next step, a DVS-BCB insulation layer is spun and a contact window is opened above the SOI waveguides. The native oxide from the exposed InAlAs layer is removed by a 20-s dip in $\text{NH}_4\text{OH} : \text{H}_2\text{O} (1 : 10)$, and finally, the coplanar Schottky

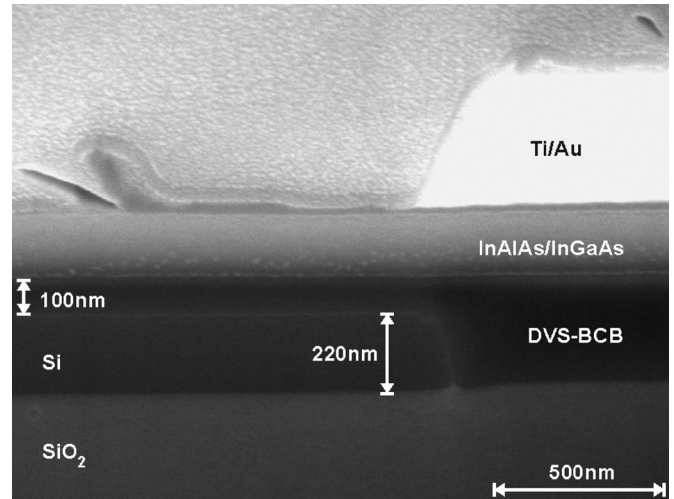


Fig. 2. Cross section of an SOI waveguide-coupled MSM detector. Only the right half of the detector/waveguide is shown in this picture.

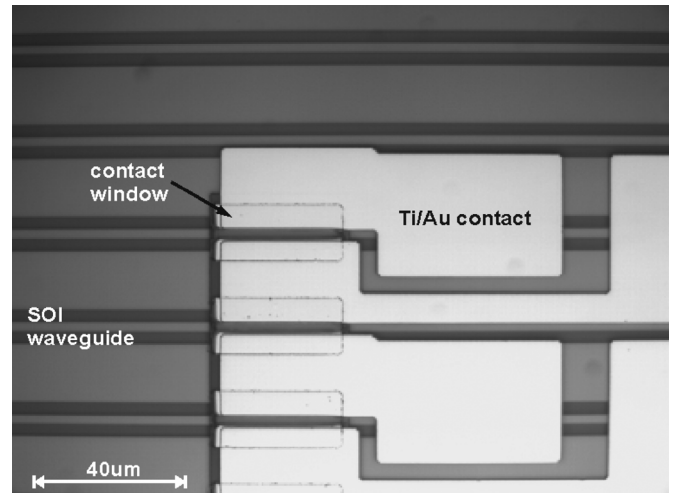


Fig. 3. Top view on three 40- μm -long thin-film MSM detectors on top of 3- μm -wide SOI waveguides. The waveguide pitch is 30 μm .

contacts are defined. Fig. 3 shows some fabricated devices with a pitch of 30 μm . These detectors are 40 μm long.

III. MEASUREMENT RESULTS

We measured MSM detectors with lengths ranging from 40 μm down to 25 μm and Schottky contact spacing of 3 μm . All these detectors were processed on top of a 3- μm -wide deeply etched SOI waveguide with a height of 220 nm. Light was coupled from a standard single-mode fiber into a 10- μm -wide ridge waveguide using shallowly etched fiber couplers [9]. The measured coupling efficiency of these fiber couplers was 25% at 1.57 μm and 21% at 1.55 μm . These waveguides are then tapered down to 3- μm -wide waveguides using adiabatic tapers. All waveguide structures, including the fiber couplers, are designed for TE-polarized light. If needed, a polarization diversity configuration can be implemented to obtain polarization-insensitive photonic integrated circuits [10].

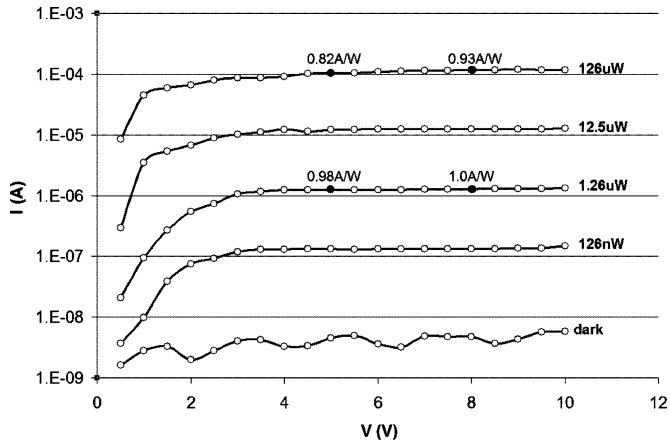


Fig. 4. I - V characteristics of a 30- μm -long detector at a wavelength of 1.55 μm . The measured dark current and photocurrents for different SOI waveguide powers are plotted. Optical power is increased in steps of 10 dB.

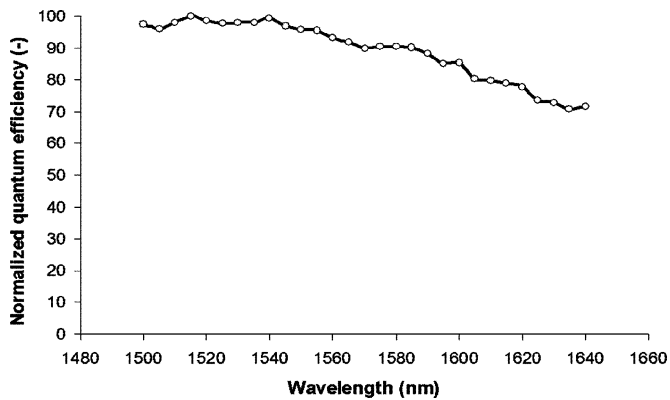


Fig. 5. Normalized QE as a function of wavelength for a 25- μm -long detector.

Fig. 4 shows the dc current-voltage (I - V) characteristics of a 30- μm -long thin-film MSM detector for different illumination conditions and a wavelength of 1.55 μm . The dark current of the device was 4.5 nA at a bias voltage of 5 V. The power coupled into the fiber was varied from 600 nW up to 600 μW in steps of 10 dB. Taking into account a fiber coupler efficiency of 21%, the SOI waveguide power varied from 126 nW up to 126 μW . The losses in the 3- μm -wide waveguides can be neglected because of their low propagation loss (~ 0.1 dB/cm) and the short length from fiber coupler to detector (~ 500 μm including taper). The internal responsivity is shown in Fig. 4 and is 1.0 A/W at a wavelength of 1.55 μm , corresponding with an internal quantum efficiency (QE) of 80%. This responsivity showed no major change for different detectors lengths ranging from 25 to 40 μm . These measurement results are in good comparison with previous reported simulation results [4].

As can be seen in Fig. 4, small saturation effects are visible at higher optical power levels due to carrier screening effects. At a waveguide power of 126 μW , the saturation is 0.8 dB at 5-V bias and 0.3 dB at 8-V bias.

For the measurement of the spectral response, light was launched into a cleaved SOI facet using a lensed fiber. Fig. 5

shows the QE for a 25- μm -long detector for wavelengths from 1.5 to 1.64 μm . These graphs are normalized so that maximum QE corresponds with 100%. Efficient detection is possible for wavelengths up to at least 1.65 μm , which corresponds to the bandgap wavelength of InGaAs lattice-matched to InP.

IV. CONCLUSION

We reported a compact and efficient InAlAs-InGaAs MSM photodetector suitable for integration on a nanophotonic SOI platform. The detector has a low dark current of 4.5 nA, a responsivity of 1.0 A/W at a wavelength of 1.55 μm and offers a high spectral bandwidth. The planar structure of the thin-film MSM detector results in an easy processing with only three lithography sequences. As the processing of these devices can be carried out on an SOI wafer scale, this integration technique does not compromise the advantages of silicon photonics: high volume, high yield, and low-cost manufacturing.

ACKNOWLEDGMENT

The authors would like to thank L. Van Landschoot for the focused ion beam cross section view and S. Verstuyft and J. Van den Troost for processing assistance. They would also like to acknowledge the epitaxy group at the Institute of Electronic Materials Technology in Warsaw (Poland) for the epi-structures.

REFERENCES

- [1] B. Jalali and S. Fathpour, "Silicon photonics," *J. Lightw. Technol.*, vol. 24, no. 12, pp. 4600-4615, Dec. 2006.
- [2] G. Roelkens, J. Brouckaert, D. Van Thourhout, R. Baets, R. Notzel, and M. Smit, "Adhesive bonding of InP/InGaAsP dies to processed silicon-on-insulator wafers using DVS-bis-benzocyclobutene," *J. Electrochem. Soc.*, vol. 153, pp. G1015-G1019, 2006.
- [3] A. W. Fang, R. Jones, H. Park, O. Cohen, O. Raday, M. J. Paniccia, and J. E. Bowers, "Integrated AlGaInAs-silicon evanescent racetrack laser and photodetector," *Opt. Express*, vol. 15, pp. 2315-2322, Mar. 2007.
- [4] J. Brouckaert, G. Roelkens, D. Van Thourhout, and R. Baets, "Thin film III-V photodetectors integrated on silicon-on-insulator photonic IC's," *J. Lightw. Technol.*, vol. 25, no. 4, pp. 1053-1060, Apr. 2007.
- [5] J. Brouckaert, G. Roelkens, D. Van Thourhout, and R. Baets, "Thin film InGaAs/InAlAs photodetectors integrated on a silicon-on-insulator waveguide substrate," in *33rd Eur. Conf. Optical Communication*, 2007, to be published.
- [6] G. Roelkens, J. Brouckaert, D. Taillaert, P. Dumon, W. Bogaerts, D. Van Thourhout, R. Baets, R. Notzel, and M. Smit, "Integration of InP/InGaAsP photodetectors onto silicon-on-insulator waveguide circuits," *Opt. Express*, vol. 13, pp. 10102-10108, 2005.
- [7] W. A. Wohlmuth, P. Fay, K. Vaccaro, E. A. Martin, and I. Adesida, "High-speed InGaAs metal-semiconductor-metal photodetectors with thin absorption layers," *IEEE Photon. Technol. Lett.*, vol. 9, no. 5, pp. 654-656, May 1997.
- [8] G. Roelkens, D. Van Thourhout, R. Baets, R. Notzel, and M. Smit, "Laser emission and photodetection in an InP/InGaAsP layer integrated on and coupled to a silicon-on-insulator waveguide circuit," *Opt. Express*, vol. 14, pp. 8154-8159, 2006.
- [9] W. Bogaerts, D. Taillaert, B. Luyssaert, P. Dumon, J. Van Campenhout, P. Bienstman, D. Van Thourhout, R. Baets, V. Wiaux, and S. Beckx, "Basic structures for photonic integrated circuits in silicon-on-insulator," *Opt. Express*, vol. 12, pp. 1583-1591, 2004.
- [10] D. Taillaert, H. Chong, P. I. Borel, L. H. Frandsen, R. M. De La Rue, and R. Baets, "A compact two-dimensional grating coupler used as a polarization splitter," *IEEE Photon. Technol. Lett.*, vol. 15, no. 9, pp. 1249-1251, Sep. 2003.